JOURNAL OF SOLID STATE CHEMISTRY **23**, 33–42 (1978)

Iron-Promoted Phases in the Tungsten–Oxygen System

I. J. McCOLM, R. STEADMAN, AND S. J. WILSON

School of Materials Science and Technology, University of Bradford, United Kingdom

Received January 26, 1977; in revised form June 2, 1977

An experimental survey of preparative work in the WO_3–Fe system in which temperatures up to 1100°C and pressures up to 55 kbar have been employed is presented. Two structures not usually found in the WO_3 or Fe–WO_3 system are encountered. Under the influence of high pressures the concentration of iron in an iron–tungsten bronze phase has been extended beyond the previously known limit of $Fe_{0.02}WO_3$ to approximately $Fe_{0.1}WO_3$, which has a hexagonal structure with $a = 7.422 \pm 0.003$ Å, $c = 3.766 \pm 0.002$ Å. In the absence of pressure but after long heating times at 1100°C and in the presence of small concentrations of iron, compositions close to W_5O_{14} yield a tetragonal phase $a = 23.33 \pm 0.01$ Å, $c = 3.797 \pm 0.001$ Å. The details of a single-crystal X-ray structural analysis of this phase are presented which show it to contain pentagonal and hexagonal tunnels and to be isostructural with Mo_5O_{14} as seen in [001] projection. The space group is identified as $P42_1m$ which is different from that of Mo_5O_{14}. The difference between W_5O_{14} and Mo_5O_{14} is seen in the presence of less severe puckering and a simpler arrangement of the metal atoms about $z = \frac{1}{2}$ which does not give rise to a superlattice cell hence leading to the observed difference in space group.

Introduction

The reaction occurring between iron and WO_3 is quite limited, requires a temperature in excess of 1000°C, and the products depend on the total amount of iron present (*1*, *2*). With very small amounts of iron $0 < x < 0.02$–0.03 in Fe_xWO_3 there is unambiguous evidence for the formation of an iron–tungsten bronze with either the orthorhombic symmetry (*1*) or tetragonal symmetry (*2*) associated with high-temperature forms of WO_3. These bronzes are ternary phases and do contain iron(II) in tunnels in the WO_3 structure. Above this low-limiting iron composition the reaction is one of reduction producing $FeWO_4$ and one of the known binary tungsten oxides. In the course of extensive studies on the Na_xWO_3–Fe system which will be reported in a later communication, we were surprised to find that a reaction began at relatively low temperatures, i.e., <500°C. Frequently amongst the products of this reaction was a hitherto unknown phase in terms of the X-ray powder pattern that it produced. The need to identify this phase prompted a more detailed examination of the Fe–WO_3 system, the results of which are reported below and show that two new structure types can be produced from WO_3 in the presence of iron.

Experimental Details

Unless otherwise stated the specimens were prepared from high-purity WO_3 (Johnson and Matthey specpure grade), tungsten and iron powders 99.99% pure (Koch Light Ltd.), and $FeWO_4$ 99.9% pure (Cerac Chemicals Ltd.) encapsulated, after mixing, in fused quartz ampoules in vacuo better than 10^{-5} Torr.

The samples for high-pressure preparation were enclosed in platinum foil and then protected from the close-fitting tantalum heater by

0022-4596/78/2312-0033 $02.00/0

a cylinder of mica. The heater and sample assembly was enclosed in a pyrophyllite tetrahedron and simultaneously heated and pressurized on the tetrahedral anvil apparatus of Standard Telephone Laboratories Ltd., Harlow.

All samples were examined by conventional optical microscopic techniques using a Zeiss Ultraphot optical microscope, and small samples from each were examined on an IRDAB Hägg–Guinier X-ray camera using CuKα_1 radiation and calibrated with KCl $a_0 =$ 6.2919 Å.

The Weissenberg technique with copper $K\alpha$ radiation was employed for all single-crystal X-ray investigations. Intensities were obtained from a Joyce–Loebl double-beam recording microdensitomer. All computing used the X-ray 74 system (*26*).

Results

Hexagonal Bronze

Reactions carried out in vacuo in the temperature range 850–1150°C for x in the range 0–0.4 in Fe_xWO_3 produced, with one notable exception which will be discussed in detail below, results exactly analogous to earlier studies (*1*, *2*). Thus only a low-x tungsten bronze, $FeWO_4$, and recognizable oxides of tungsten were present in the phase mixtures after long (3 weeks) or short (8 hr) heating times.

The reaction conditions were extended when a high-pressure apparatus was made available. Sample FM9 prepared at 55 kbar and 1300°C with a composition $Fe_{0.100}WO_3$, whilst containing a small amount of $FeWO_4$, was predominantly a phase with the hexagonal tungsten bronze structure $a = 7.422$ Å, $c = 3.766$ Å which is prima facie evidence for having extended the iron content considerably beyond that attainable under less vigorous conditions. The hexagonal symmetry of this phase is unexpected since it is a structure usually associated with bronzes containing relatively large cations such as potassium or rubidium. It is clearly a metastable phase since annealing under vacuum at 850°C leads to decomposition and the appearance of $W_{18}O_{49}$ as the main product. Nevertheless, the application of high pressure and the presence of Fe has given rise to an unexpected tungsten oxide structure. To date the same conditions applied to WO_3 without the iron, while producing as yet unidentified structures, do not lead to a hexagonal phase, and therefore it seems that we have prepared a hexagonal iron bronze that would not be expected from ion size considerations.

Tetragonal Oxide

It was mentioned above that an exceptional result was obtained whilst surveying the Fe–WO_3 system. This occurred while attempting to prepare $Fe_{0.3}WO_3$ from WO_3 + W and material certified as $FeWO_4$ by the supplier. Pelleted material of alleged $Fe_{0.3}WO_3$ composition heated at 600°C for 3 weeks and then 1000°C for 1 week produced a purple-colored coarsely crystalline material. Microscopic examination showed two distinct phases, bluish-purple acicular crystals and finely divided black material. The X-ray powder pattern showed the presence of $FeWO_4$ plus a strong sharp pattern that arose clearly from the phase observed weakly in the Na–Fe–WO_3 work. Furthermore, the acicular crystals could be easily separated out and single-crystal examination showed them to have tetragonal symmetry with a unit cell that could account for all the non-$FeWO_4$ lines in the powder pattern. The sharpness of the X-ray powder lines contrasts strongly with the diffuse patterns obtained from reduced tungsten trioxide phases. Only the $FeWO_4$ used in this preparation was different from all earlier attempts, and so this was more closely examined. X-ray analysis showed it to be largely amorphous with a few weak δ-FeOOH lines. Mössbauer spectral analysis showed the iron to be in the ferric state, and acid leaching with HNO_3 left a yellow residue of 70.4 wt% WO_3. Thermal analysis showed a 10.4% weight loss between 120 and 440°C and it was concluded that, far from being $FeWO_4$, it was a mixture of

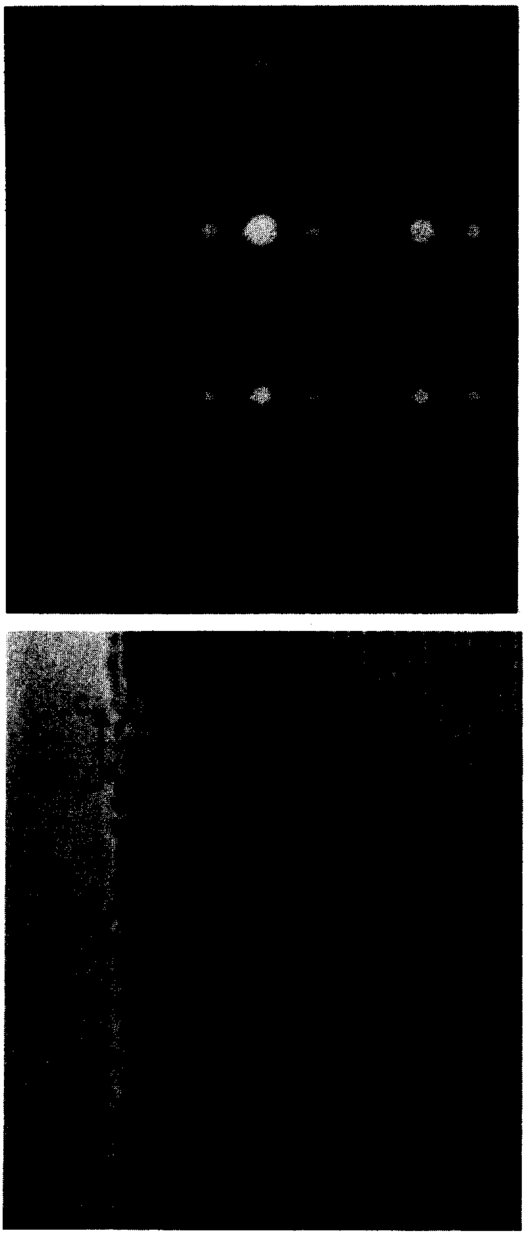

FIG. 1. (Upper) Electron diffraction pattern; and (lower) micrograph from crystals of W_5O_{14}.

hydrated ferric oxide and WO_3 with a composition $Fe_2O_3 2.5WO_3 4.8H_2O$. On this basis the bronze sample attempted earlier had been $Fe_{0.22}WO_{3.03} 0.54H_2O$ and the presence of water must have subjected the sample to hydrothermal pressure conditions during the preparation. This probably accounts for the obvious crystallinity of the material and for many explosive failures during this part of the experimental work. While further attempts were made to prepare the new phase as a single product, advantage was taken of the availability of well-formed single crystals from this preparation for a single-crystal X-ray and electron microscope investigation.

A characteristic micrograph and diffraction pattern from the electron microscope are shown in Fig. 1, lattice fringes with approximately 11-Å spacing are clearly seen. Two prominent reciprocal-lattice spacings in the electron diffraction pattern corresponded to 3.8 and 22 Å and were used as a basis for considering the X-ray powder data already collected for the sample. Thus the X-ray powder pattern was indexed on the basis of a tetragonal cell with $a = 23.33 \pm 0.01$ Å and $c = 3.797 \pm 0.001$ Å.

This pattern is presented in Table I where it has been indexed taking account of the systematic absences found in the single-crystal X-ray analysis reported below. It was recognized that the pattern in Table I was similar to that published for Mo_5O_{14} (*12*) and if one assumed that the preparation was a mixture in which all the iron was present as $FeWO_4$ then the acicular crystals would have a composition $WO_{2.75}$. In the presence of H_2O vapor, this might easily be $WO_{2.8}$ and so be the analog of Mo_5O_{14}. The X-ray single-crystal examination confirmed that the unknown and Mo_5O_{14} were indeed isostructural in two-dimensional [001] projection, and it was felt then that this was the first time such a structure had been proved to exist in the tungsten–oxygen system. However, it has since been first reported by others (*13*, *14*).

The wide range of sample compositions and preparation conditions used in attempts to isolate the phase are shown in Table II together with the results obtained. It is interesting to see that monophasic material was only obtained for the composition $(Fe_{0.01}W_{0.99})_5O_{14}$, which is further confirmation of the idea that a new tungsten oxide W_5O_{14} had been prepared in the presence of iron. Because of the small

TABLE I

W_5O_{14}: X-RAY POWDER DIFFRACTION PATTERN, $CuK\alpha_1$ RADIATION[a]

I	d (obs, Å)	$\sin^2\theta \times 10^4$ (obs)	hkl	$\sin^2\theta \times 10^4$ (calc)	I	d (obs, Å)	$\sin^2\theta \times 10^4$ (obs)	hkl	$\sin^2\theta \times 10^4$ (calc)
11	11.62	44	200	44	42	2.630	858	541	858
18	10.38	55	210	55	3	2.576	894	910	894
7	7.404	108	310	109	10	2.564	903	631	902
5	5.846	174	400	174	3	2.528	929	920 760	927
14	5.515	195	330	196	13	2.489	958	551 711	956
4	5.220	218	420	218	15	2.463	978	641	978
4	4.579	283	510	283	~7	2.448	990	721	989
3	4.338	315	520	316	3	2.383	1045	731	1044
3	4.133	347	440	349	~3	2.369	1057	940	1057
25	3.888	393	600	392	4	2.313	1109	801	1109
4	3.840	402	610	403	30	2.303	1119	811 741	1120
100	3.803	410	001	411	6	2.268	1154	821	1153
4	3.688	436	620	436	6	2.228	1195	661	1196
~40	3.645	447	540	447	8	2.207	1218	751	1218
4	3.612	455	201	455	6	2.195	1231	870	1232
4	3.571	465	211	466	4	2.166	1264	10.40	1264
15	3.477	491	630	491	3	2.130	1308	911	1305
5	3.381	519	311	520	3	2.087	1362	11.20 10.50	1363
16	3.303	544	550 710	545	7	2.046	1417	9.70 11.30	1417
16	3.236	567	640	567	6	1.944	1570	12.00	1570
11	3.203	578	720	578	4	1.937	1581	12.10 980	1581
3	3.184	585	401	586	4	1.918	1614	12.20	1613
8	3.128	606	331	608	~3	1.909	1628	10.70	1624
6	3.068	630	421 730	629 632	48	1.898	1647	871 002	1643 1646
5	2.917	697	800	698					
43	2.895	708	810 740	709					
5	2.829	741	820	741					
4	2.795	760	441	760					
10	2.747	786	660	785					
20	2.714 2.710	805 808	601 750	804 807					
6	2.696	816	611	815					
4	2.648	846	821	847					

[a] Tetragonal, $a = 23.33 \pm 0.01$ Å; $c = 3.797$ Å.

amount of iron present it is not possible to say whether or not it is incorporated into the structure. It seems from the tabulated results that the phase appears after relatively long heating times at high temperatures and with small amounts of iron in the system. However, it must be emphasized that since the first crystalline sample came from a high iron

TABLE II

FE–W–O SAMPLES

Sample	Composition	Treatment (°C)	Phase analysis: Microscope	Phase analysis: X-ray	Lattice parameters (Å)
1	approx. $Fe_{0.22}WO_{3.03}$ $+0.54\ H_2O$	600° 520 hr 1000° 168 hr	purple-blue acic. Xtline, black met. mat.	s W_5O_{14} s $FeWO_4$	$a = 23.33$ $c = 3.797$
6	$WO_{2.792} + 0.043\ FeWO_4$ from Fe; W; WO_3	850° 142 hr	dk. blue powdery	s $W_{18}O_{49}$ reduced WO_3	
8		1000° 92 hr	dk. blue polycrystalline; some needles	s $W_{18}O_{49}$ reduced WO_3	
FM7		55 kbar 750° $\frac{3}{4}$ hr	blue-grey compact mat. contg. some gold metallic fragments	complex WO_3-type	
9	$WO_{2.800} + 0.314\ FeWO_4$ from $FeWO_4$; W; WO_3	1000° 120 hr ~18 atm H_2O	blue-black acicular Xtlline + black met. mat.	s complex WO_3-type mw $FeWO_4$	
3	$(Fe_{0.553}W_{17.531})O_{49}$ or $Fe_{0.158}W_{5.009}O_{14}$ from Fe_2O_3; W; WO_3	700° 19 hr 850° 46 hr	dk. blue powdery	s $W_{18}O_{49}$ mw $FeWO_4$ Fe_2O_3	
10		1000° 96 hr ~16 atm H_2O	blue-black acicular crystalline	s complex WO_3-type vw $FeWO_4$	
11		1000° 1034 hr	mauve-blue fibrous and acic.	s $W_{18}O_{49}$ w $FeWO_4$ w Fe_2O_3	
4	$(Fe_{2.011}W_{16.000})O_{49}$ from Fe_2O_3; W; WO_3	700° 19 hr 850° 46 hr	blue-grey powdery	s complex WO_3-type m $FeWO_4$	
	$(Fe_{0.050}W_{4.950})O_{14}$ from Fe; W; WO_3	1100° 8 hr	dk. blue fibrous and acic.	complex WO_3-type	
15		1100° 168 hr	purple-blue fibrous	W_5O_{14} only	$a = 23.32$ $c = 3.795$
16		1100° 4 weeks	purple-blue finely fibrous	W_5O_{14} only	$a = 23.31$ $c = 3.795$
5	$(Fe_{0.191}W_{4.810})O_{14}$ from Fe; W; WO_3	850° 142 hr	blue powdery	complex WO_3-type	
7		850° 46 hr ~42 Torr H_2O	blue fibrous	complex WO_3-type	
12		1000° 1034 hr	dk. blue and fibrous acic.	complex WO_3-type	
2	$Fe_{0.019}WO_3$ from Fe; WO_3	850° 333 hr	grey-green polycrystalline and some larger crystals	orthorh. WO_3-type phase	$a = 7.354$ $b = 7.450$ $c = 3.857$

TABLE II—*Continued*

Sample	Composition	Treatment (°C)	Phase analysis		Lattice parameters (Å)
			Microscope	X-ray	
FM9	$Fe_{0.100}WO_3$ from $FeWO_4$; W; WO_3	55 kbar ~1300° 1 hr	purplish and gold compact polycrystalline	s hexag. bronze phase w $FeWO_4$ ms WO_2	$a = 7.422$ $c = 3.766$
13		FM9 heated 850° 92 hr	compact mauve finely fibrous and black met.	s $W_{18}O_{49}$ w $FeWO_4$ w WO_2	

TABLE III[a]

W_5O_{14}: THREE-DIMENSIONAL STRUCTURE

Space group	:	$P\bar{4}2_1m$	No. 113
Unit cell	:	$a = 23.33$	$c = 3.797$ Å
Unit cell content	:	$8W_5O_{14}$	
8W and 16O in 6 × 4(*e*)	:	$x, \frac{1}{2}+x, z;$	$\bar{x}, \frac{1}{2}-x, z;$
		$\frac{1}{2}+x, x, \bar{z};$	$\frac{1}{2}-x, x, \bar{z}.$
32W and 96O in 16 × 8(*f*)	:	$x, y, z;$	$\frac{1}{2}-x, \frac{1}{2}+y, \bar{z};$
		$\bar{x}, \bar{y}, z;$	$\frac{1}{2}+x, \frac{1}{2}-y, \bar{z};$
		$\bar{y}, x, \bar{z};$	$\frac{1}{2}+y, \frac{1}{2}+x, z;$
		$y, \bar{x}, \bar{z};$	$\frac{1}{2}-y, \frac{1}{2}-x, z.$

Atom	Pos.[n]	*x*	*y*	*z*	*U* (Å²)
W 1	4(*e*)	0.2013(3)	0.7013(3)	0.500(10)	0.0049(19)
2	4(*e*)	0.0992(3)	0.5992(3)	0.492(11)	0.0058(20)
3	8(*f*)	0.0468(3)	0.3400(3)	0.514(10)	0.0088(15)
4	8(*f*)	0.0808(3)	0.0810(3)	0.483(7)	0.0092(14)
5	8(*f*)	0.1576(3)	0.2213(2)	0.487(8)	0.0055(15)
6	8(*f*)	0.2397(3)	0.0747(3)	0.484(7)	0.0085(15)
O 7	4(*e*)	0.201(4)	0.701(4)	−0.03(9)	0.0057(18)
8	4(*e*)	0.103(4)	0.603(4)	−0.08(11)	
9	8(*f*)	0.049(3)	0.341(4)	−0.13(10)	
10	8(*f*)	0.083(4)	0.083(4)	−0.03(6)	
11	8(*f*)	0.160(4)	0.222(3)	−0.03(10)	
12	8(*f*)	0.240(4)	0.079(4)	−0.11(5)	
13	4(*e*)	0.401(4)	0.901(4)	0.59(6)	
14	4(*e*)	0.272(4)	0.772(4)	0.43(7)	
15	8(*f*)	0.263(4)	0.002(4)	0.50(4)	
16	8(*f*)	0.012(3)	0.083(4)	0.58(6)	
17	8(*f*)	0.094(3)	0.145(3)	0.57(7)	
18	8(*f*)	0.097(4)	0.282(4)	0.55(6)	
19	8(*f*)	0.176(4)	0.052(4)	0.45(5)	
20	8(*f*)	0.198(5)	0.184(4)	0.82(4)	
21	8(*f*)	0.314(4)	0.094(4)	0.46(5)	
22	8(*f*)	0.384(3)	0.032(3)	0.61(10)	

[a] $R = 0.107$.

content preparation, and subsequent attempts to use water vapor and repeat this preparation have failed, the preparative conditions leading to formation of this phase and the role of the iron are not understood.

Single-Crystal X-Ray Structural Analysis of W_5O_{14}

A small needle-shaped crystal that could be approximated to a cylinder with radius 0.0137 mm and length 0.14 mm was used. The needle axis was found to coincide with the tetragonal *c*-axis. Using the equiinclination Weissenberg method the *hk*0, *hk*1, and *hk*2 layers of the reciprocal lattice were recorded and, after remounting, 00*l* reflections were also recorded.

None of the X-ray photographs showed any evidence for the existence of a superlattice, and the 23.33 × 3.797 Å unit cell found in the powder data was taken as the true unit cell. The Laue symmetry was 4/*mmm*. The presence of the following reflections was noted: *hkl* all orders, *hk*0 all orders, *hhl* all orders, *h*0*l* all orders, *h*00 for *h* even, and 00*l* all orders. The class *h*0*l* with *h* odd is represented by just one reflection (502). In the absence of this it would be possible to choose a space group *P*4/*mbm* with a mirror plane so that all the tungsten atoms would lie at $z = \frac{1}{2}$. However, the reflection (502) is definitely present but since this is the only one in this class it emphasizes that only a small deviation from coplanarity of the W atoms exists.

The presence of only one observed reflection in the *h*0*l* class with *h* odd gives rise to speculation that this may be the result of a double diffraction effect. However, the 502 reflection did not look out of place in the pattern as far as intensity profile and spot shape are concerned when it might do so if arising from the Renninger effect. In the *hk*2 Weissenberg layer both 502 and 052 reflections were present whilst no pair of strong allowed reflections appears to exist in the X-ray powder pattern that could combine to give these. Furthermore, even when fixing one W atom at $Z = \frac{1}{2}$ in the more general space group it would not refine the remaining W atoms to $z = \frac{1}{2}$. In the light of these findings the space group *P*4/*mbm* was felt to be less likely than $P42_1m$ or $P42_12$.

Of the two possible space groups $P42_1m$ and $P42_12$, only the first is compatible with the two-dimensional model for Mo_5O_{14} (*15*) and is therefore chosen.

The intensities of 428 reflections were measured and used to determine the structure with the "X-ray 74" system after taking as an initial model *x* and *y* parameters from the two-dimensional structure of Mo_5O_{14} (*15*). The first reliability value at 19% indicated the correctness of the model. A final least-squares operation with individual and overall temperature factors for tungsten and oxygen, respectively, gave an *R*-value of 10.7%. Positional and thermal parameters obtained from the procedure are given in Table III and an electron density section at $z = \frac{1}{2}$ is shown in Fig. 2. The average interatomic distances are given in Table IV with those from related structures for comparison. It can be seen that the average displacement of W from $z = \frac{1}{2}$ is only 0.043 Å.

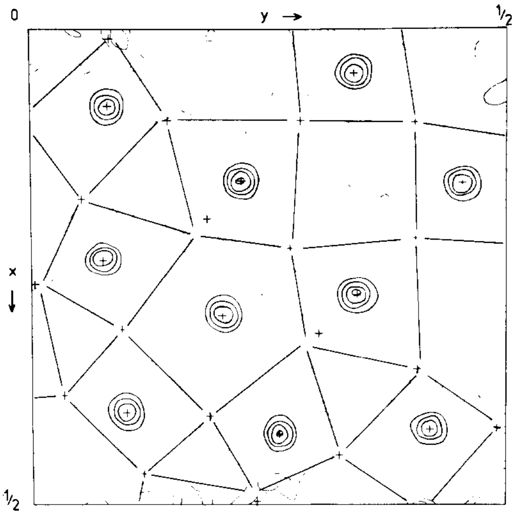

FIG. 2. Electron density section at $z = \frac{1}{2}$ of one-quarter of the unit cell of W_5O_{14}. Contours are at 50, 100, 150, 200 $e^-/Å^3$ for W atoms and at 10 and 20 $e^-/Å^3$ for other peaks. Atomic positions given by three-dimensional refinement are marked +.

TABLE IV

AVERAGE INTERATOMIC DISTANCES FOR W_5O_{14}

W–O in octahedra = 1.950 Å
(cf. 1.91 for tetrag. K_xWO_3 (*24*) and the ranges 1.79–2.10 and 1.84–2.00 Å found for $Na_{0.33}WO_3$ and $Na_{0.48}WO_3$ (*23*), respectively).

Equatorial W–O in pentag. site = 2.548 Å
(cf. for Mo–O the ranges 1.94–2.03 in $Mo_{17}O_{47}$ (*20*) and 2.01–2.09 in $(Ta,Mo)_5O_{14}$ (*21*)).

W–W : pentagon–octahedron = 3.307 Å
(cf. the range 3.31–3.44 in $W_{18}O_{49}$ (*25*)).

Equatorial W–W : between octahedra = 3.783 Å
(cf. the range 3.62–3.96 in $W_{18}O_{49}$ (*25*), average displacement of W atoms from $z = \frac{1}{2} = 0.043$ Å).

A two-dimensional projection revealed that each of the equatorial O–W–O angles in the pentagonal column are within 1° of 72°, which emphasizes the geometrical regularity of this structural feature.

Discussion

The appearance of a hexagonal Fe_xWO_3 phase containing Fe with $0.10 > x > 0.03$ in a high-pressure sample is enteresting since this structure is usually associated with large cations such as Rb^+, K^+, Cs^+ (*3*), Tl^+ (*4*), NH_4^+ (*5*), and In^+ (*6*, *7*), and the Fe^{2+} cation is considerably smaller than any of these. It should be noted, however, that cation size is probably of less importance in determining symmetry under high-pressure conditions since a number of other investigations using high-pressure or hydrothermal conditions have produced evidence for a hexagonal bronze from a range of differing sized cations, e.g., Li^+ (*8*), Na^+ (*9*), Ba^{2+}, Ca^{2+}, Sr^{2+} (*10*). The unit cells found for hexagonal bronze phase are in the range $a = 7.31$–7.50 Å, $c = 7.43$–7.63 Å. In these examples a doubled c-axis was shown to be present, but there is no evidence for such doubling in the X-ray diffraction lines for this iron sample with c found to be 3.766 Å. However, its cell parameters do fall well within the observed ranges for hexagonal tungsten bronzes if the c-axis is doubled, and so this lends support to its assignment as a hexagonal tungsten bronze. There could, however, be a slight doubt about this conclusion if the decomposition to $W_{18}O_{49}$ is thought to be of importance. Pseudohexagonal Mo-doped oxides have been reported (*11*) with compositions $MoW_{11}O_{36}$, $MoW_{14}O_{45}$. Compounds of this type and composition have empty tunnel sites, and hence their lattice parameters differ considerably at $a = 7.29$ Å, $c = 3.834$ Å from the range quoted for hexagonal bronzes. Furthermore, since many other attempts aimed at producing iron-substituted tungsten oxides have failed, it seems that this phase is a hexagonal iron-tungsten bronze.

W_5O_{14}

While the structural analysis revealed some interesting differences with respect to the coplanarity of the W in W_5O_{14} and Mo atoms in Mo_5O_{14} the preparative work is revealing with respect to their relative stabilities. Mo_5O_{14} occurs as a metastable phase in the Mo–O binary system when prepared below 530°C but just prolonged heating at these low temperatures results in decomposition to $Mo_{17}O_{47}$ and MoO_3 (*12*, *16*). In contrast W_5O_{14} occurs after long heating times at temperatures above 1000°C and although the conditions required for its formation are not well understood, its appearance after such treatments does not suggest metastability or easy decomposition. Mo_5O_{14} can be stabilized by partial substitution of the Mo and so $(Mo_{1-x}T_x)O_{2.8}$ with $x = 0.04$ for $T = Ti$ (*17*), $x = 0.09$ and 0.40 for Nb, $x = 0.07$ for Ta (*18*), and $0.02 \leqslant x \leqslant 0.11$ for V (*16*) can be prepared up to 760°C without signs of decomposition on prolonged heating. These more stable substituted Mo_5O_{14} phases have been studied and compared to the parent material. Kihlborg (*15*) first studied the structure of Mo_5O_{14} and noted the doubled a-axis parameter indicated by additional diffuse reflections in the upper Weissenberg layers with $l = 0$. The structure of the subcell was solved in projection down the *c*-axis to give *x*- and *y*-parameters for Mo and oxygen atoms in the two-dimensional space group *p4g*. Systematic absences in the superlattice reflections gave *P4/n* as the probable three-dimensional space group. However, the diffuseness of these reflections indicated partial disorder of the *z* parameters and precluded a full structure determination. The Mo atoms were assumed to form a puckered layer with $z = \pm 0.425$ by analogy with the structure of $Mo_{17}O_{47}$ (*19*, *20*). The tantalum-doped material $(Mo_{0.93}Ta_{0.07})_5O_{14}$ produced sharper superlattice reflections and a lesser degree of disorder in the structure (*21*). A two-dimensional refinement showed that all the Ta atoms occupy pentagonal column sites. The arrangement of the puckered Mo atom layer in the Ta-doped crystal was such as to give a superlattice cell with orthorhombic symmetry $Pb2_1a$ with $a = 45.75$ Å, $b = 22.87$ Å, $c = 4.002$ Å. The extent of the puckering effect can be estimated from the lattice parameter changes, as substitution of small amounts of Ti, V, Nb, or Ta into Mo_5O_{14} leads to an increase in the *c* parameter but a decrease in the tetragonal subcell *a* parameter caused by a greater degree of puckering. Doping with tungsten has the opposite effect (*22*), and extrapolation of Ekstrom's data on W-doped Mo_5O_{14} to W_5O_{14} supports the conclusion that very little W puckering occurs in this phase since the lattice parameters found in this work fit the long extrapolated lines in Fig. 3 quite well. This feature is the principal difference between Mo_5O_{14} and W_5O_{14} structures where in the Ta-doped Mo_5O_{14} the average displacement of Mo atoms from $z = \frac{1}{2}$ is determined to be 0.348 Å whereas in W_5O_{14} it is only 0.043 Å. Such variation in puckering amplitude seems to be a general feature of the differences between Mo and W oxides. Thus in $Mo_{17}O_{47}$ the average displacement from $z = \frac{1}{2}$ is 0.298 Å (*20*), in $Na_{0.33}WO_3$ it is 0.060 Å, while in $Na_{0.48}WO_3$ (*23*), tetragonal K_xWO_3 (*24*, *27*), and $W_{18}O_{49}$ (*25*) it is 0.

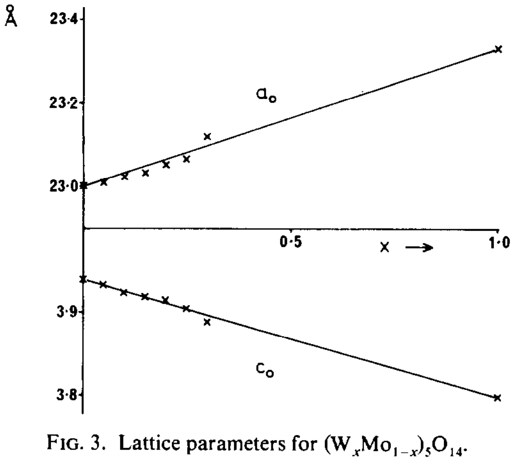

FIG. 3. Lattice parameters for $(W_xMo_{1-x})_5O_{14}$.

Since the identification of this phase in the Fe–W–O system and the elucidation of its structure here other workers have found it to exist also in the Ge–W–O system (*13*) and in a wide range of preparations with general composition $M_{0.02}W_{0.98}O_{2.80}$ where M = Li, Na, K, Rb, Cs, Mg, Ba, Mn, Fe, Cu, Zn, Cd, In, Sn, Bi (*14*). Since these cationic species bear little relation to each other in terms of valence or ionic size it might best be assumed that the phase is in fact a binary tungsten oxide, the formation of which is catalyzed or promoted in some way by the presence of foreign ions. In all cases the preparation conditions were 1 week at 1100°C in vacuo which is in accord with the conditions found most suitable for the Fe–W–O system in this work.

In summary it appears that the presence of iron ions together with high pressure and temperature lead to a hexagonal form of WO_3 that is in fact a tungsten bronze phase. Furthermore, the presence of iron ions and temperatures around 1100°C can lead to the formation of a tetragonal W_5O_{14} oxide of tungsten that has been shown to be different from the Mo_5O_{14} structure only in the degree of displacement of the W atoms from coplanarity compared to the Mo atoms in Mo_5O_{14}.

Acknowledgments

The support of the Science Research Council through a studentship to S.J.W. and a grant to use high-pressure facilities at S.T.L. Ltd., Harlow is gratefully acknowledged. We thank Mr. J. Penfold of S.T.L. for practical help and Dr. R. J. D. Tilley for assistance with the electron microscopy and general discussion of these systems. S.J.W. was also in receipt of a Bradford University studentship.

References

1. I. J. McColm, R. J. D. Tilley, C. P. M. Barton, and N. N. Greenwood, *J. Solid State Chem.* **16**, 265 (1976).
2. J. P. Doumerc, G. Schiffmacher, P. Caro, and M. Pouchard, *C.R. Acad. Sci. Ser. C* **282**, 295 (1976).
3. A. Magneli and B. Blomberg, *Acta Chem. Scand.* **5**, 372 (1951).
4. M. S. Whittingham and L. D. Clark, *J. Chem. Phys.* **53**, 4114 (1970).
5. P. G. Dickens, A. C. Halliwell, D. J. Murphy, and M. S. Whittingham, *Trans. Faraday Soc.* **67**, 794 (1971).
6. R. J. Bouchard and J. L. Gillson, *Inorg. Chem.* **7**, 969 (1968).
7. A. B. Swanson and J. S. Anderson, *Mater. Res. Bull.* **3**, 149 (1968).
8. T. E. Gier, D. C. Pease, A. W. Sleight, and T. A. Bither, *Inorg. Chem.* **7**, 1646 (1968).
9. T. A. Bither, J. L. Gillson, and H. S. Young, *Inorg. Chem.* **5**, 1559 (1966).
10. P. E. Bierstedt, T. A. Bither, and F. J. Darnell, *Solid State Commun.* **4**, 25 (1966).
11. J. Graham and A. D. Wadsley, *Acta Crystallogr.* **14**, 379 (1961).
12. L. Kihlborg, *Acta Chem. Scand.* **13**, 954 (1959).
13. T. Ekstrom, E. Iguchi, and R. J. D. Tilley, *Acta Chem. Scand. A* **30**, 312 (1976).
14. T. Ekstrom and R. J. D. Tilley, *J. Solid State Chem.* **19**, 125 (1976).
15. L. Kihlborg, *Ark. Kemi* **21**, 427 (1963).
16. T. Ekstrom and M. Nygren, *Acta Chem. Scand.* **26**, 1827 (1972).
17. T. Ekstrom, *Acta Chem. Scand.* **26**, 1843 (1972).
18. T. Ekstrom and N. Nygren, *Acta Chem. Scand.* **26**, 1836 (1972).
19. L. Kihlborg, *Acta Chem. Scand.* **14**, 1612 (1960).
20. L. Kihlborg, *Acta Chem. Scand.* **17**, 1485 (1963).
21. N. Yamazoe and L. Kihlborg, *Acta Crystallogr. Sect. B* **31**, 1666 (1975).
22. T. Ekstrom, *Mater. Res. Bull.* 7, 19 (1972).
23. F. Takusagawa and R. A. Jacobson, *J. Solid State Chem.* **18**, 163 (1976).
24. L. Kihlborg and A. Klug, *Chem. Scr.* **3**, 207 (1973).
25. A. Magneli, *Ark. Kemi* **1**, 223 (1949).
26. "X-ray system June 1974," Technical Report TR-192 Computer Science Center, University of Maryland.
27. A. Magneli, *Ark. Kemi* **1**, 213 (1949).